A Proposed Model of Bradykinin Bound to the Rat B2 Receptor and Its Utility for Drug Design

Donald J. Kyle,* Sarvajit Chakravarty, Jacqueline A. Sinsko, and Thomas M. Stormann

Scios Nova Inc., 6200 Freeport Centre, Baltimore, Maryland 21224

Received August 5, 1993•

A putative model of bradykinin bound to the rat B2 receptor was generated using a combination of homology modeling (from the known transmembrane structure of bacteriorhodopsin), energy minimization, molecular dynamics, and a two-stage conformational search as a docking simulation. Overall, the proposed bound ligand adopts a twisted "S" shape, wherein a C-terminal β-turn is buried in the receptor just below the extracellular boundary of the cell membrane and the N-terminus is interacting with negatively charged residues in extracellular loop 3 of the receptor (most notably Asp^{268} and Asp^{286}). Mutagenesis experiments describing mutations which result in both a loss of bradykinin affinity as well as those which have no effect on bradykinin affinity are in good agreement with the proposed structure. In short, the mutagenesis results and the computational simulations each point to the same region of the receptor as likely to bind bradykinin. A double mutation, predicted as being likely to have a dramatic effect on bradykinin binding affinity, was confirmed experimentally, adding some validation to the proposed complex. Moreover, a new pseudopeptide bradykinin receptor antagonist (D-Arg^0-Arg^1-[12-aminododecanoyl]^2-Ser^3-D-Tic^4-Oic^5-Arg^6) was designed on the basis of the model, and found to have good receptor affinity. Speculation regarding other possible sites for mutagenesis are also described.

Introduction

Bradykinin (Arg^1-Pro^2-Pro^3-Gly^4-Phe^5-Ser^6-Pro^7-Phe^8-Arg^9) is a linear nonapeptide hormone generated by the action of kallikrein on kininogen, a high molecular weight precursor protein. Once released, bradykinin is able to elicit a wide variety of pathophysiological responses including pain and inflammation.[1] Because of its central role in so many disorders, there might be great commercial value in a bradykinin receptor antagonist which is potent, competitive, selective for the receptor, and orally bioavailable. Although no compounds meeting all of these criteria have yet been reported, there has been a recent description of a non-peptide bradykinin antagonist,[2] and there have been steady advances in the development of peptide receptor antagonists.

The two most typical examples of these new peptide antagonists are HOE 140 (D-Arg^0-Arg^1-Pro^2-Hyp^3-Gly^4-Thi^5-Ser^6-D-Tic^7-Oic^8-Arg^9)[3] and NPC 17731 (D-Arg^0-Arg^1-Pro^2-Hyp^3-Gly^4-Phe^5-Ser^6-D-Hype(trans propyl)^7-Oic^8-Arg^9).[4] The latter peptide is a member of a series of peptides for which extensive structure–activity information has been developed about the C-terminal portion. More recently, N-terminally cyclized peptide antagonists of similar sequences have been described, providing further insight into the biologically active conformation of these peptides.[5] The advent of these new conformationally constrained peptides has provided valuable information about the steric and electrostatic requirements of the receptor for ligand binding. Ideally, in addition to this indirectly obtained information, one would like to have a model of bradykinin bound to its receptor as an aid in drug design. Unfortunately, due to the nature of this receptor, it has not yet been obtained in crystalline form, nor is it likely to be in the near future.

The bradykinin receptor is a member of a family of receptors for which an intracellular interaction with a G-protein is a critical part of the signal transduction pathway following agonist binding. Recently, bradykinin B2 receptors were cloned and sequenced from both rat and human.[6,7] Structurally, these G-protein-coupled receptors extend from beyond the extracellular boundary of the cell membrane into the cytoplasm. The tertiary structure is such that the protein crosses the bilayer of the cell membrane seven times, thus forming three intracellular loops and three extracellular loops and having cytoplasmic C-terminal and extracellular N-terminal strands. It is generally accepted that the transmembrane domains of these receptors exist as a bundle of helical strands.[8] This assumption is derived primarily on the known structure of the transmembrane portions of a structurally related protein, bacteriorhodopsin.[9]

Knowledge about the three-dimensional structure of a receptor–ligand complex can be of significant value in the design of new antagonists. However, G-protein-coupled receptors do not lend themselves to analysis by either NMR or X-ray crystallography due to their structural dependence on an intact cell membrane. Our approach toward obtaining this valuable structural information is based on structural homology modeling, molecular dynamics, and systematic conformational searching methods. The combination of these techniques led to the proposed model of bradykinin bound to its receptor that we present herein. Support for this model is presented in the form of correlation with site-directed-mutagenesis data, as well as in the predictive capabilities of the model. For example, we show experimentally that a double mutation predicted by the model as being likely to cause a dramatic loss in bradykinin binding affinity does so. In addition, we report for the first time a pseudopeptide antagonist designed from the proposed model. Aside from its interesting properties as a bradykinin receptor antagonist, the ability to use a receptor model, such as the one proposed, for new compound design illustrates the overall value of such models, even though they are highly speculative in the absence of support from either NMR or X-ray crystallography.

• Abstract published in *Advance ACS Abstracts*, April 1, 1994.

0022-2623/94/1837-1347$04.50/0

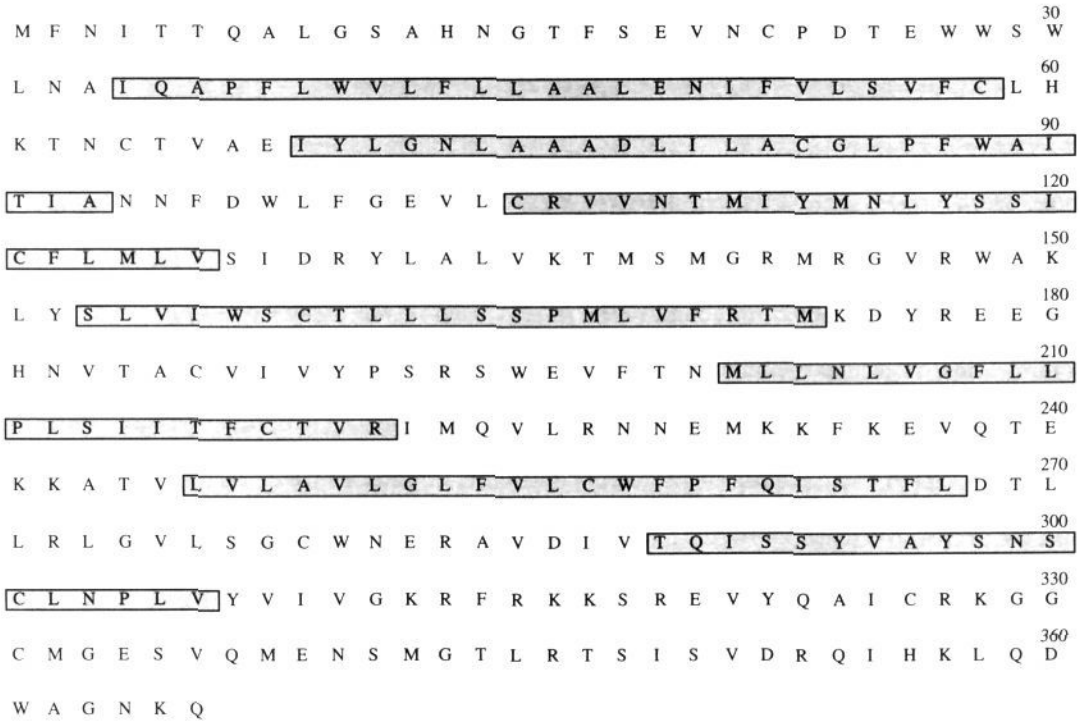

Figure 1. Primary amino acid sequence of the rat B2 bradykinin receptor. Amino acids proposed to be part of the seven transmembrane domains are highlighted.

Methods

A. General Computational Procedures. All calculations were performed on a Silicon Graphics 4D480 workstation using custom routines written using the program CHARMm,[10] version 22, using the default charges and parameters. Throughout the calculations a constant dielectric equal to 1 was used since the receptor core is envisioned predominantly as a hydrophobic environment. The cutoff distance for generating the nonbonded list was set to 15 Å. During calculations, either molecular dynamics or energy minimization, the non-bonded list was updated every 20 steps. The integration time step used for the molecular dynamics calculations was 0.001 ps step^{-1}. Computational results were graphically rendered using the program QUANTA, version 3.3.[11]

B. Model Construction. A hydropathicity (Kyte–Doolittle) calculation[12] on the amino acid sequence of the rat bradykinin receptor yielded seven segments, each of which were 21–25 contiguous residues with predominantly hydrophobic side chains. These were presumed to be the seven transmembrane portions of the receptor. The amino acid sequence of the rat bradykinin B2 receptor is shown in Figure 1 together with the zones selected as the transmembrane portions. Cartesian coordinates of the backbone atoms within each of these seven segments were *built by structural homology from the cryomicroscopic* structure of the analogous segments of a related protein, bacteriorhodopsin.[9] Subsequently, side chains were added to these seven segments as appropriate for the rat bradykinin receptor, and the resulting geometry was optimized via constrained energy minimization to alleviate bad contacts. The resulting helices were oriented such that, for the most part, hydrophobic residues were oriented outward. Extracellular and intracellular loops were extracted from the Protein Data Bank library, following a geometric search based upon a vector defined by terminal α carbons in adjacent helices.

There are four Cys residues in the extracellular loop region of the rat bradykinin B2 receptor which might form a disulfide bond(s). Although there is some evidence for a disulfide bond in non-peptide-activated G-protein-*coupled receptors where ligand binding is exclusively* transmembrane, there is no experimental evidence for an extracellular loop disulfide(s) in the rat bradykinin B2 receptor where our data suggests that the extracellular loop three plays a role in binding. In the absence of experimental support, no extracellular loop disulfide bonds were incorporated into this model.

All backbone atoms within this initial model were subsequently constrained in a harmonic fashion (force constant = 5 kcal Å^{-1} mol^{-1}), and the entire structure was subjected to 500 steps of steepest descents followed by 2000 steps of Adopted-Basis Newton Raphson energy minimization. The constrained geometry optimization was performed to alleviate bad steric contacts introduced during the side-chain growth steps of the homology procedure. Next, all constraints were removed and the minimization procedure was repeated in an unconstrained fashion. Finally, an unconstrained (50 ps) molecular dynamics simulation was carried out at 300 K and, from the final 20 ps of the coordinate trajectory, an average structure of the receptor was extracted. The overall *potential energy of this structure was minimized exhaus*tively (2000 steps of Adopted-Basis Newton Raphson energy minimization) with no constraints. The resulting structure of the receptor was used in all subsequent docking calculations.

C. Docking Procedure. Following the literature precedent that bradykinin adopts a C-terminal β-turn upon complexation with the receptor,[13,14] the ϕ, ψ backbone dihedral angles in the tetrapeptide Ser-Pro-Phe-Arg were constrained in a harmonic fashion (force constant = 15 kcal Å^{-1} mol^{-1}) to values which define a β-turn.[15] This tetrapeptide probe was then systematically translated

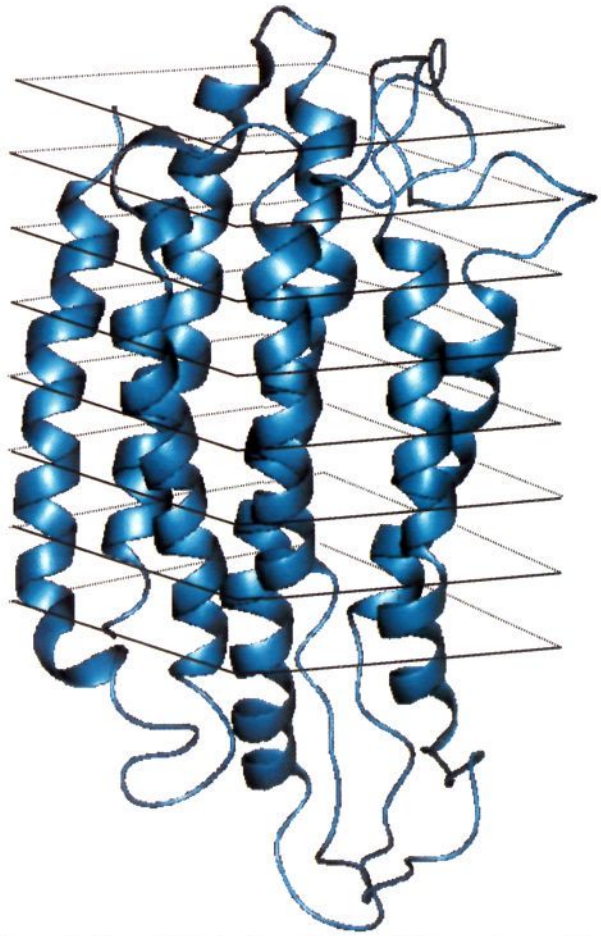

Figure 2. Overall illustration of the rat B2 receptor model (blue). Shown in black is an illustrative representation of the horizontal planes, separated by 3Å, within which the tetrapeptide probe (Ser-Pro-Phe-Arg) was translated about in a 3Å × 3Å grid pattern.

about the interior of a theoretical box inscribing the rat receptor model, the plane of the probe's β-turn being roughly perpendicular to the axes to of the transmembrane domains of the receptor. The box encompassed the entire receptor with the exception of the intracellular loops (where agonist binding is not likely) and the outermost portions of the extracellular loops. The translations were such that the tetrapeptide probe molecule was incrementally repositioned within the receptor by following a 3Å × 3Å × 3Å grid pattern as schematically shown in Figure 2. At each new position, both the probe and receptor were reset to their initial conformations, then the geometry of the complex was optimized using 200 steps of steepest descents followed by 500 steps of Adopted-Basis Newton Raphson energy minimization. The overall structural integrity of the receptor was maintained by applying weak harmonic constraints (force constant = 15 kcal $Å^{-1}$ mol^{-1}) to the backbone atoms during the procedure. These constraints were such that the receptor backbone would have some flexibility while attempting to accommodate the probe molecule, but not so much flexibility that it could be structurally disrupted by the attempted optimization of a very poor initial probe–receptor complex (e.g. When the tetrapeptide probe was initially placed directly on top of a transmembrane helix). Conceptually, these constraints on the backbone atoms of the receptor might serve a purpose similar to that of the cell membrane in providing overall stability, with some limited flexibility to the receptor. The side chains of the amino acids in the ligand and the receptor were always allowed to be completely flexible. The probe molecule was free to tumble at each new point within the receptor during geometry optimization, in accordance with the steric topology of the receptor. Hence, although initially perpendicular to the receptor's transmembrane helical axes, the plane of the probe's β-turn after geometry optimization was highly variable. Subsequently, the sum of the steric and electrostatic contributions to the overall potential energy (interaction energy) as measured only between the tetrapeptide probe molecule and the atoms of the receptor was calculated. A representative horizontal slice through the receptor, illustrating the energy of interaction as gray scale contour lines, is shown in Figure 3a (darker gray = lower interaction energy). An analogous representation for the complete portion of receptor which was sampled by the tetrapeptide probe molecule is shown as an edge-on, frontal view in Figure 3b, where it is qualitatively clear where the transmembrane domains are located (white), as well as where the most favorable sites of probe interaction are located (black). This type of stacked, shaded contour plot is a highly effective and novel means of studying the topology of these types of receptor models.

This initial stage of the docking process was used to reduce the computational difficulties which would be inherent in "tumbling" a complete bradykinin molecule with great flexibility about the receptor in a similar fashion. However, following this initial stage, insight into those regions of the receptor capable of accommodating the C-terminal portion of the bradykinin molecule was obtained. On the basis of energetics and as qualitatively shown in Figure 3b, those particular regions are clustered in the central part of the receptor near the extracellular domain. Using this information as a steering device to limit the size of the problem, an exhaustive conformational search was performed using the entire nine residue sequence of bradykinin as a probe molecule, again enforcing a C-terminal β-turn via dihedral angle constraints. Specifically, 24 unique geometric orientations (eight on each of the three axes) of the bradykinin molecule were sampled at each of 100 grid points identified during the initial stage as likely zones to bind the tetrapeptide probe molecule. These ligand orientations were defined as a 90° rotation about a given axis (x, y, or z) of the approximate plane of the β-turn, directed toward both positive and negative values of each axis (x, y, or z). Thus, there were eight orientations aligned on each of the three primary axes. Overall, 2400 unique possibilities of bradykinin bound to receptor were taken as starting points for subsequent geometry optimization and computation of an energy of interaction.

Optimized bradykinin–receptor complexes with interaction energies not greater than 150 kcal mol^{-1} above the lowest found were considered as the most likely candidates for a good model. Within this 150 kcal mol^{-1} window, there were 17 complexes. Table 1 summarizes the ϕ, ψ backbone dihedral angles of bradykinin in each of the 17 complexes, together with the corresponding bradykinin internal energy and the overall interaction energy for each complex.

The interaction energies calculated for these 17 complexes were significantly lower than those determined for the remaining 2383 complexes, the best of which was still

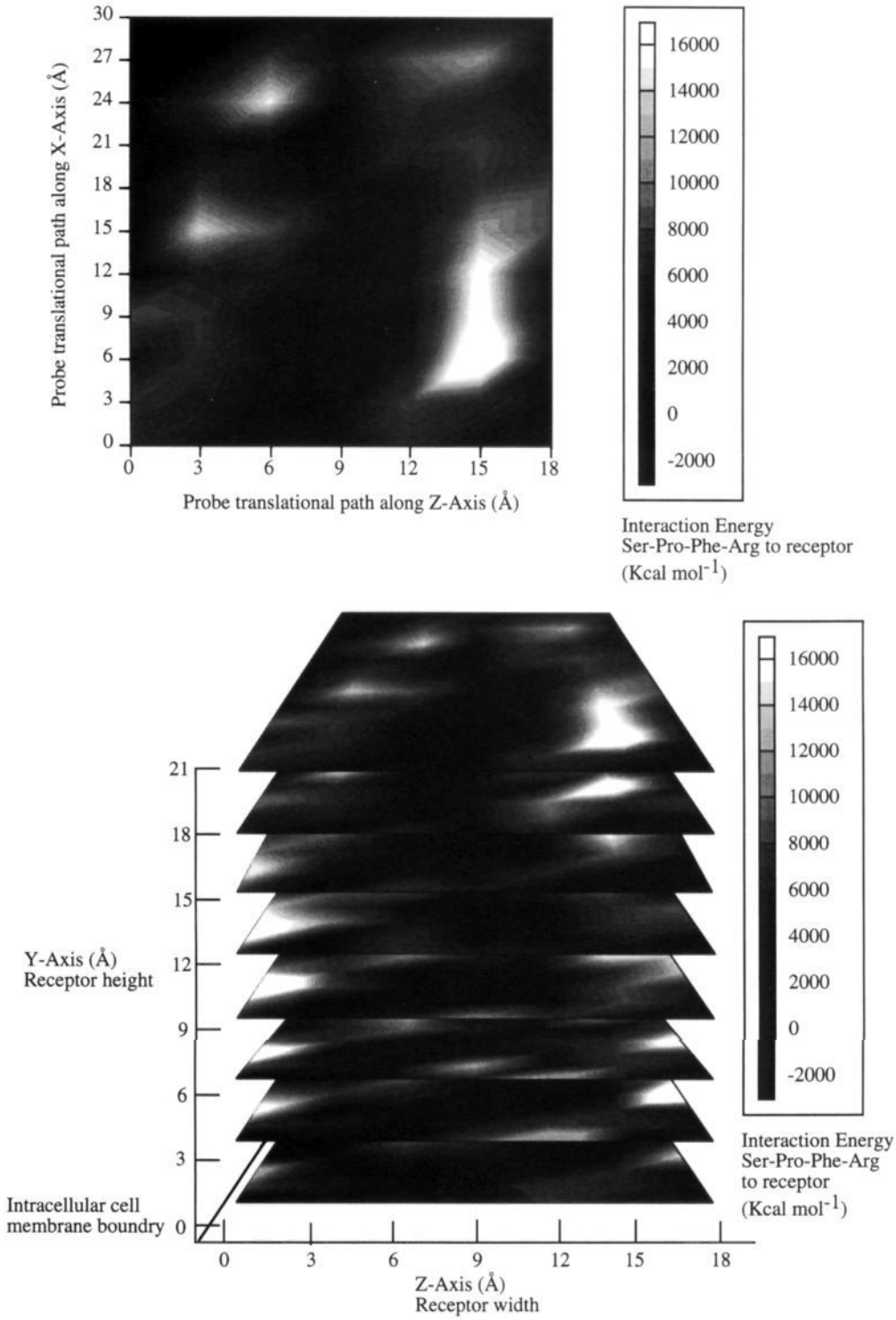

Figure 3. (a) Representative contour plot showing energy of interaction between tetrapeptide probe (Ser-Pro-Phe-Arg) and rat B2 receptor model. This plot represents a horizontal slice across the transmembrane domain of the receptor, approximately 18 Å up from the intracellular membrane boundary, within which the tetrapeptide probe was translated in a 3Å × 3Å fashion. Darker contours indicate most favorable interaction and the lightest contours represent least favorable interactions, i.e. the locations of the transmembrane helices. (b) Contour plots showing energy of interaction between probe and receptor. Each contour plot corresponds to horizontal slices depicted in Figure 2. Darker gray indicates most favorable interaction, and the light shades represent least favorable interactions, i.e. locations of the transmembrane helices.

ca. 200 kcal mol^{-1} higher than complex **I** (the highest energy structure of the 17 shown in Table 1). Ultimately, complex **XVI** was selected as the proposed model on the basis of its agreement with our mutagenesis experiments (next section). With respect to energetics, this complex was ranked second in terms of interaction energy and 10th in terms of bradykinin internal energy. This represents good agreement with logic in that one would not necessarily expect the lowest energy conformation of isolated bradykinin to be the same as the receptor-bound conformation, but the ligand–receptor interaction for this complex appears to be comparatively optimal.

Table 1. Energetic and Structural Data Corresponding to the 17 Bradykinin-Receptor Complexes of Lowest Interaction Energy

		ϕ (deg) / ψ (deg)									
complex	Arg	Pro	Pro	Gly	Phe	Ser	Pro	Phe	Arg	complex interaction energy (kcal/mol)	bradykinin internal energy (kcal/mol)
I		−10.8	−80.1	163.7	123.4	−118.6	−31.1	−70.9	−174.8	−252.4	−57.0
	132.3	−169.8	−131.5	−130.8	−122.9	142.2	−57.4	−38.5			
II		−110.1	−31.7	−155.2	−165.3	−169.1	−23.9	−69.7	−170.1	−253.4	−98.7
	−163.3	173.3	173.2	173.6	−75.3	114.5	−50.7	−34.1			
III		−75.3	−105.3	83.1	−169.5	106.8	−44.4	−52.1	−160.5	−254.7	−33.3
	94.7	−105.2	−171.2	143.5	75.5	116.0	−65.9	−15.9			
IV		−58.9	−40.8	−167.0	178.9	148.5	−34.9	−67.2	170.2	−257.8	13.1
	−133.1	134.6	−150.2	172.8	−3.8	132.0	−56.8	−47.4			
V		0.8	−121.6	−171.1	174.6	−139.6	−28.3	−58.5	−170.0	−259.8	−38.5
	−145.2	−114.6	132.4	−157.0	−93.8	133.7	−47.8	−36.0			
VI		−4.7	−53.2	161.6	−133.1	−137.6	−23.7	−82.3	−166.8	−259.8	−81.5
	138.6	−174.2	−168.2	155.9	−76.9	135.4	−60.3	−41.6			
VII		−38.2	18.0	73.0	−142.1	88.1	−31.4	−88.1	179.1	−259.9	−73.7
	176.2	161.3	129.3	−154.4	146.0	127.2	−63.5	−42.3			
VIII		−126.8	−21.4	−175.2	102.8	66.4	−22.8	−70.4	−175.7	−261.9	−30.2
	−88.6	−162.2	157.6	173.7	33.5	116.7	−53.4	−36.6			
IX		−33.4	18.8	−57.3	−137.5	77.5	−12.8	−76.5	−166.2	−266.5	75.4
	−80.4	−176.1	10.9	178.8	26.8	127.4	−63.1	−32.9			
X		−69.7	−21.6	−165.5	−81.3	117.3	−26.6	−62.9	170.1	−268.9	114.5
	174.4	−18.5	147.2	161.5	−37.7	128.7	−84.4	−33.9			
XI		−70.9	−95.2	132.4	136.4	152.9	−38.8	−70.4	178.6	−270.2	20.7
	−171.5	−144.9	−138.9	−116.5	46.7	124.5	−69.6	−42.5			
XII		−49.0	−33.7	−168.5	−150.0	52.6	−32.1	−51.1	−169.4	−271.1	−103.7
	162.6	165.0	148.9	163.0	98.2	117.8	−37.1	−34.7			
XIII		−33.2	−105.1	−113.4	−173.2	77.6	−23.1	−89.9	179.7	−273.2	140.3
	−151.7	140.9	−156.7	124.6	56.9	116.9	−65.4	−43.9			
XIV		−76.8	−37.6	−178.9	−147.0	−143.7	−35.2	−55.7	−172.5	−288.4	−4.6
	93.8	−90.5	81.6	175.4	−105.9	134.9	−68.9	−26.5			
XV		−83.6	−0.4	−130.9	172.5	123.6	−31.5	−65.9	−174.7	−297.7	5.5
	−177.5	169.6	165.7	151.8	−19.9	116.8	−58.9	−29.7			
XVI		−99.2	−98.3	170.3	−136.6	167.8	−42.7	−65.8	−163.7	−298.9	−23.3
	144.7	157.1	155.6	−147.6	−75.7	141.0	−76.9	−28.4			
XVII		−19.8	−63.1	−157.0	−161.9	79.3	−45.1	−70.5	−173.6	−371.8	−32.5
	104.2	170.9	156.1	163.3	13.3	126.9	−45.1	−37.3			

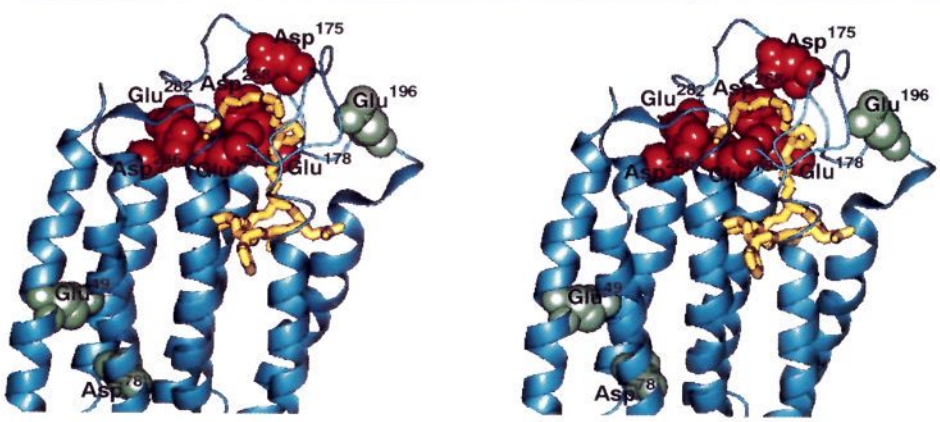

Figure 4. Selected, proposed model of bradykinin bound to the rat B2 receptor. Receptor is shown in blue, and the bradykinin backbone and side-chain atoms are shown in yellow. Point mutations having no significant adverse effects on bradykinin binding are colored green. Mutation clusters affecting bradykinin binding are shown in red.

Results and Discussion

A. Final Model Selection. As an aid in the selection of which of the bradykinin–receptor complexes to consider our "lead" model, supporting experimental evidence was sought from site-directed-mutagenesis experiments. This support was taken primarily from recent work describing bradykinin binding assays performed on mutant rat bradykinin B2 receptors.[16] In that work, each receptor contained either a point mutation or a small cluster of point mutations wherein native residues having negatively charged side chains (Asp, Glu) were replaced by alanine-(s). Figure 4 shows the selected ligand–receptor complex (XVI) chosen on the basis of best agreement with the results of these mutagenesis studies. Overall, there is excellent agreement with this experimental data and the selected, proposed model of bradykinin bound to its receptor. None of the other putative complexes were in as good agreement with this experimental data and were not considered further. Of particular significance in the work was that the transmembrane residue Glu^{49}, when mutated to alanine, showed no adverse effect on bradykinin receptor affinity with respect to the rat wild type. A similar result was reported for the $Glu^{196} \rightarrow Ala^{196}$ mutation. These residues are remotely situated with respect to the proposed site of bradykinin binding. In contrast, the [Asp^{175},-$Glu^{178,179}$] → $Ala^{175,178,179}$ cluster mutation showed a 12-fold loss in bradykinin binding affinity, and the [Glu^{282}, Asp^{286}] → $Ala^{282,286}$ cluster mutation lost 17-fold with

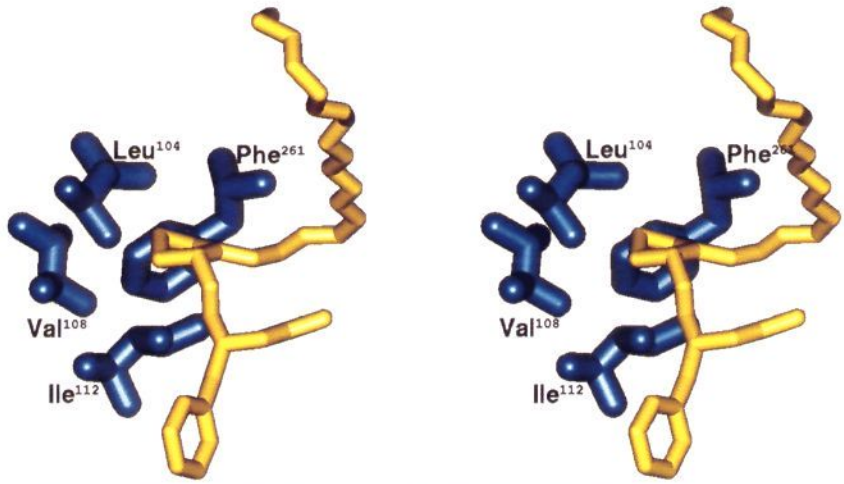

Figure 5. Primary residues in the receptor forming a hydrophobic cavity (blue) about Pro^7 of bradykinin (yellow) in the proposed model.

respect to the wild type receptor. Asp^{268} → Ala^{268} and Asp^{286} → Ala^{286} point mutations caused 19- and 28-fold respective losses in affinity for bradykinin. These residues are located within the receptor model at positions directly adjacent to the proposed site of bradykinin binding. All of these mutant receptors were demonstrated to be functional receptors on the basis of bradykinin-induced chloride channel activation in an oocyte expression system.[16]

The selected model is characterized by an overall twisted "S"-shaped ligand, similar to the conformation of bradykinin determined previously in a hydrophobic environment by NMR.[13] One interesting observation is that the side chains of both Phe^5 and Phe^8 extend into hydrophobic clefts between transmembrane helices. Specifically, the Phe^5 side chain is positioned within the space between transmembranes 5 and 6. The Phe^8 side chain extends similarly between transmembranes 3 and 4. These side chains do not protrude out into what might be considered the membrane environment. Overall, the model suggests that the N-terminal amino and guanidine groups of Arg^1 interact directly with negatively charged amino acids in extracellular loop 3, and the C-terminal end is in a β-turn conformation buried just below the extracellular boundary of the transmembrane domain of the receptor. Noteworthy, is the presence of a hydrophobic cavity in our receptor model located adjacent to Pro^7 of the bradykinin ligand. This cavity is made up, in part, by the residues Phe^{261}, Leu^{104}, Val^{108}, and Ile^{112} as shown in Figure 5. Given the historical significance of position 7 in peptide bradykinin-like ligands, these residues represent interesting targets for further mutagenesis experiments. One such result, the mutation of Phe^{261} to Ala^{261}, has already been described.[17] This point mutation, located in the midst of the hydrophobic cavity, dramatically reduces the ability of bradykinin to bind to this receptor. This result is in agreement with our proposed model. A recent publication describing a mutagenesis study of the substance P receptor, another peptide hormone-activated, G-protein-coupled receptor, also implicated extracellular loop 3 of the receptor in ligand binding.[18]

B. Model Validation. In addition to the correlation with site-directed-mutagenesis data as previously described, a model such as the one proposed here can also, within reasonable limits, be validated by its predictive capabilities. Close inspection of the bradykinin Arg^1 side-chain location and surrounding receptor interactions led to the suspicion that Asp^{286} and Asp^{268} might be jointly interacting either with the guanidino group in the side chain of Arg^1 or the N-terminal amino group in bradykinin. Mutagenesis experiments[15] showed that replacing either Asp^{268} or Asp^{286} with an alanine in mutant receptors caused 19- and 28-fold (respectively) losses in bradykinin binding affinity. However, if the suspected triad electrostatic interaction were accurate, then a receptor containing a double mutation (Asp^{268,286} → Ala^{268,286}) should show a much more dramatic loss in affinity for bradykinin than would receptors containing the individual point mutations. The appropriate double-mutation experiment confirmed this in that the double-mutant-containing receptor showed a 500-fold loss in affinity for bradykinin, as predicted.[15] This type of an ionic interaction is also precedented by the body of literature which exists supporting the requirement of an N-terminal arginine residue and free N-terminal amino group in both bradykinin peptide agonists and antagonists for high-affinity binding.[19]

Further consideration of the model presented here led to the hypothesis that, perhaps, antagonist peptides bind in a similar fashion, although not likely identically to bradykinin. Moreover, it was thought that all that may be required for binding is an intact C-terminal β-turn structure with appropriate side chains in place and N-terminal amino and guanidine groups for primary electrostatic interaction(s) with Asp^{286} and Asp^{268} in extracellular loop 3. As a test of this hypothesis, the prototypical second-generation antagonist **I** (D-Arg^0-Arg^1-Pro^2-Hyp^3-Gly^4-Phe^5-Ser^6-D-Tic^7-Oic^8-Arg^9) was modified such that the Pro^2-Hyp^3-Gly^4-Phe^5 section was replaced by a simple 12-carbon chain spacer (12-aminododecanoic acid). The resulting compound, **II**, contains only the appropriately charged moieties at the N-terminus, separated by a simple organic spacer moiety from a known β-turn forming tetrapeptide.[20] As summarized in Table 2, this pseudopeptide was tested in the classical bradykinin B_2 receptor binding assay[21] and found to have a K_i of 360 nM against [^{3}H]bradykinin. In addition, the compound is a functional antagonist as measured in guinea pig ileum against bradykinin-induced contraction (pA_2 = 5.5).[22]

This new pseudopeptide represents a substantial pharmaceutical improvement over the 10-residue-containing parent peptide in that it is a much less peptidic molecule, containing only three natural amino acids. In the overall

Table 2. Bradykinin Antagonist Pseudopeptide in Vitro Pharmacology

peptide	amino acid sequence[a]	guinea pig ileum K_i (nM)	guinea pig ileum pA_2
I	D-Arg^0-Arg^1-Pro^2-Hyp^3-Gly^4-Phe^5-Ser^6-DTic^7-Oic^8-Arg^9	0.11 ± 0.21 (3)	8.8
II	D-Arg^0-Arg^1-(12-aminododecanoyl)^2-Ser^3-DTic^4-Oic^5-Arg^6	360 ± 8.30 (3)	5.5

[a] D-Tic corresponds to the D stereoisomer of tetrahydroisoquinolinecarboxylic acid, and Oic corresponds to octahydroindolecarboxylic acid. Hyp corresponds to 4-hydroxyproline.

strategy for converting the decapeptide antagonist into a non-peptide, this first example of a third-generation bradykinin antagonist represents substantial progress. Taking this new molecule as a lead structure, together with the receptor model and structure–activity relationship associated with related compounds including cyclic antagonists, we are pursuing the synthesis of several related pseudopeptides which are expected be more potent and, perhaps, will show oral activity.

In conclusion, it is important to note that the construction of a model, such as the one described in this report, of a G-protein-coupled receptor with a flexible nonapeptide ligand bound is an extraordinary computational problem with very little prior precedent. Although it correlates well with relevant experimental results, much of the model is speculative and can only be confirmed by subsequent crystallography or NMR experiments. This type of experimentally determined structural information is not attainable using current technologies, so one must rely only upon the best "proposed models" that can be built, which incorporate as much experimental data as possible (i.e. mutagenesis and structure–activity relationship (SAR) in ligands). We have demonstrated one approach toward addressing this difficult problem and have shown via the discovery of compound **II** that even a relatively crude model can be of tremendous value in the drug discovery process. That progress can be attributed to the effective integration of many disciplines including synthetic chemistry, computational chemistry, and molecular biology.

Experimental Section

General. A. Synthesis. All peptides were synthesized manually according to standard techniques using *tert*-butyloxycarbonyl amino acids.[24] All amino acids were purchased from Bachem Bioscience Inc., with the exception of Boc-Oic-OH, which was synthesized according to previously reported procedures.[25] Boc-protected 12-aminododecanoic acid was prepared from the corresponding free amine (Aldrich) using standard techniques. Boc-Arg(Tos)-Pam resin (0.6 mmol/g) was purchased from Applied Biosystems (Foster City, CA) and used for the synthesis. Syntheses were run on 0.5-g resin-amino acid (0.3 mmol) scales and couplings were monitored using qualitative ninhydrin determination of free amine (Kaiser test). The finished peptidyl-resin was washed and dried in vacuum to a constant weight and then treated with anhydrous hydrogen fluoride (in the presence of 10% anisole) at 10 mL/g of peptidyl-resin for 1 h at 0 °C. After removal of the HF the resin peptide was washed extensively with ether (3 × 20 mL) and then extracted with 0.1% TFA. The crude material obtained after lyophilization was purified using reverse-phase HPLC, using a linear gradient of 5–60% water/acetonitrile (both containing 0.1% TFA). The homogeneous pooled pure fractions were lyophilized, and the purity of the white fluffy powders was determined by fast atom bombardment mass spectroscopy and analytical reverse-phase high-performance liquid chromatography. These analytical results are summarized in Table 3.

H-D-Arg-Arg-Pro-Hyp-Gly-Phe-Ser-D-Tic-Oic-Arg-OH. The peptide was synthesized manually according to standard techniques, using *tert*-butyloxycarbonyl amino acids. All protected amino acids were purchased from Bachem Bioscience Inc.

Table 3. Experimentally Determined Analytical Data for Peptides I and II

peptide	fast atom bombardment MS $[M + H]_{calc}$	fast atom bombardment MS $[M + H]_{obs}$	analytical HPLC[a] t_R (min)
I	1298	1298	16.04
II	1082	1082	17.52

[a] C_{18} Vydac analytical column, 22.5 cm × 4.6 mm i.d. linear gradient of water/acetonitrile (both containing 0.1% TFA) 5–80% acetonitrile over 30 min at 1 mL min^{-1}. Detector set to 220 nM.

Boc-Oic-OH was synthesized according to previously reported procedures.[25] Boc-Arg(Tos)-Pam resin (0.6 mmol/g) was purchased from Applied Biosystems (Foster City, CA) and used for the synthesis. The synthesis was run using 0.5 g resin-amino acid (0.3 mmol), and couplings were monitored using qualitative ninhydrin determination of free amine (Kaiser test). The finished peptidyl-resin was washed and dried to a constant weight and then treated with anhydrous hydrogen fluoride (in the presence of 10% anisole) at 10 mL/g of peptidyl-resin for 1 h at 0 °C. After removal of the hydrogen fluoride, the resin peptide was washed extensively with ether (20 mL × 3) and then extracted with 0.1% TFA. The crude material obtained after lyophilization was purified using reverse-phase high-performance liquid chromatography, using a linear gradient of 5–60% water/acetonitrile (both containing 0.1% TFA). The homogenous pooled pure fractions were lyophilized, and the purity of the white fluffy powders was determined by fast atom bombardment mass spectroscopy and analytical reverse-phase high-performance liquid chromatography.

H-D-Arg-Arg-(12-aminododecanoyl)-Ser-D-Tic-Oic-Arg-OH. The peptide was synthesized manually according to standard techniques, using *tert*-butyloxycarbonyl amino acids.[24] All protected amino acids were purchased from Bachem Bioscience Inc. Boc-Oic-OH was synthesized according to previously reported procedures.[25] The 12-aminododecanoic acid was Boc protected according to standard procedures.[26] Boc-Arg(Tos)-Pam resin (0.6 mmol/g) was purchased from Applied Biosystems (Foster City, CA) and used for the synthesis. The synthesis was run using 0.5 g resin-amino acid (0.3 mmol), and couplings were monitored using qualitative ninhydrin determination of free amine (Kaiser test). The finished peptidyl-resin was washed and dried to a constant weight and then treated with anhydrous hydrogen fluoride (in the presence of 10% anisole) at 10 mL/g of peptidyl-resin for 1 h at 0 °C. After removal of the hydrogen fluoride, the resin peptide was washed extensively with ether (3 × 20 mL) and then extracted with 0.1% TFA. The crude material obtained after lyophilization, was purified using reverse-phase high-performance liquid chromatography, using a linear gradient of 5–60% water/acetonitrile (both containing 0.1% TFA). The homogenous pooled pure fractions were lyophilized, and the purity of the white fluffy powders was determined by fast atom bombardment mass spectroscopy and analytical reverse-phase high-performance liquid chromatography.

Acknowledgment. The authors would like to express their sincere gratitude to Diedre Wilkins for performing the receptor binding assay on the pseudopeptide reported in this manuscript.

References

(1) Kyle, D. J.; Burch, R. M. A Survey of Bradykinin Receptors and Their Antagonists. *Curr. Opin. Invest Drugs* **1993**, *2* (1), 5–20.
(2) Saluino, J. M.; Seaane, P. R.; Douty, B. D.; Awad, M. M. A.; Dolle, R. E.; Houck, W. T.; Faunce, D. M.; Sawutz, D. G. Design of potent non-peptide competitive antagonists of the human bradykinin B2 receptor. *J. Med. Chem.* **1993**, *36*, 2583–2584.

(3) (a) Hock, F. J.; Wirth, K.; Albus, U.; Linz, W.; Gerhards, H. J.; Wiemer, G.; Henke, St.; Breipohl, G.; Knoig, W.; Knolle, J.; Sholkens, B. A. HOE 140 a New Potent and Long Acting Bradykinin Antagonist: In Vitro Studies. *Br. J. Pharmacol.* **1991**, *102*, 769–773. (b) Wirth, K.; Hock, F. J.; Albus, U.; Linz, W.; Alperman, H. G.; Anagnostopoulos, H.; G.; Henke, St.; Breipohl, G.; Knoig, W.; Knolle, J.; Sholkens, B. A. HOE 140 a new potent and long acting bradykinin antagonist: In vivo studies. *Br. J. Pharmacol.* **1991**, *102*, 774–777.

(4) Kyle, D. J.; Martin, J. A.; Burch, R. M.; Carter, J. P.; Lu, S.; Meeker, S.; Prosser, J. C.; Sullivan, J. P.; Togo, J.; Noronha-Blob, L.; Sinsko, J. A.; Walters, R. F.; Whaley, L. W.; Hiner, R. N. Probing the Bradykinin Receptor: Mapping the Geometric Topography Using Ethers of Hydroxyproline in Novel Peptides. *J. Med. Chem.* **1991**, *34*(8), 2649–2653.

(5) Chakravarty, S.; Wilkens, D.; Kyle, D. J. Design of Potent, Cyclic Peptide Bradykinin Receptor Antagonists From Conformationally Constrained Linear Peptides. *J. Med. Chem.* **1993**, *36* (17), 2569–2571.

(6) McEachern, A. E.; Shelton, E. R.; Bhakta, S.; Obernolte, R.; Bach, C.; Zuppan, P.; Fujisaki, J.; Aldrich, R. W.; Janigan, K. *Proc. Natl. Acad. Sci. U.S.A.* **1991**, *88*, 7724–7728.

(7) Hess, J. F.; Borkowski, J. A.; Young, G. S.; Strader, C. D.; Ransom, R. W. Cloning and Pharmacological Characterization of a Human Bradykinin BK2 Receptor. *Biochem. Biophys. Res. Commun.* **1992**, *184*, 260–268.

(8) Hilbert, M. F.; Trumpp-Kallmeyer, S.; Bruinvels, A.; Hoflack, J. Three-Dimensional Models of Neurotransmitter G-Binding Protein-Coupled Receptors. *Mol. Pharmacol.* **1991**, *40*, 8–15.

(9) Henderson, R.; Baldwin, J. M.; Ceska, T. A.; Zemlin, F.; Beckmann, E.; Downing, K. H. Model for the Structure of Bacteriorhodopsin Based on High Resolution Electron Cryomicroscopy. *J. Mol. Biol.* **1990**, *213*, 899–929.

(10) (a) Brooks, B. R.; Bruccoleri, R. E.; Olafson, B. D.; States, D. J.; Swaminathon, S.; Karplus, M. J. CHARMM: A Program for Macromolecular Energy Minimization, and Dynamics Calculations. *J. Comput. Chem.* **1983**, *4*, 187–217. (b) Molecular Simulations, Inc. 16 New England Executive Park, Burlington, MA 01803-5297.

(11) Molecular Simulations, Inc. 16 New England Executive Park, Burlington, MA 01803-5297.

(12) Kyte, J.; Doolittle, R. F. A Simple Method for Displaying the Hydropathic Character of a Protein. *J. Mol. Biol.* **1982**, *157*, 105–132.

(13) Kyle, D. J.; Hicks, R. P.; Blake, P. R.; Klimkowski, V. J. Conformational Properties of Bradykinin and Bradykinin Antagonists. In *Bradykinin Antagonists: Basic and Clinical Research*; Burch, R. M., Ed.; Marcel Dekker: New York, 1990; pp 131–146.

(14) Lee, S. C.; Russell, A. F.; Laidig, W. D. Three Dimensional Structure of Bradykinin in SDS Micelles. *Int. J. Pept. Protein Res.* **1990**, *35*, 367–371.

(15) Rose, G. D.; Gierash, L. M.; Smith, J. A. Turns in Peptides and Proteins. *Adv. Protein Chem.* **1985**, *37*, 1–109.

(16) (a) Burch, R. M.; Kyle, D. J.; Stormann, T. M. Molecular Biological Approaches to the Study of B2 Bradykinin Receptors. In *Molecular Biology and Pharmacology of Bradykinin Receptors*; R. G. Landes Co.: Austin, 1993; pp 19–32. (b) Novotny, E. A.; Bednar, D. L.; Connolly, M. A.; Connor, J. R.; Stormann, T. M. Mutation of aspartate residues in the third extracellular loop of the rat B2 bradykinin receptor decreases affinity for bradykinin. Submitted for publication in *Mol. Pharmacol.*

(17) Freedman, R.; Jarnagin, K. Cloning of a B2 Bradykinin Receptor: Examination of the Bradykinin Binding Site by Site-Directed Mutagenesis. *Recent Progress on Kinins*; Birkhauser Verlag Basel; 1992; pp 487–496.

(18) Gether, U.; Johansen, T. E.; Snider, R. M.; Lowe, J. A.; Nakanishi, S.; Schwartz, T. W. Different Binding Epitopes for Substance P and the Non-Peptide Antagonist, CP 96, 345, on the NK_1 receptor. *Nature* **1993**, *362*, 345–348.

(19) Stewart, J. M.; Vavrek, R. J. Chemistry of Peptide B2 Bradykinin Antagonists. In *Bradykinin Antagonists: Basic and Clinical Research*; Burch, R. M., Ed.; Marcel Dekker: New York, 1990; pp 51–96.

(20) Kyle, D. J.; Blake, P. R.; Smithwick, D.; Green. L. M.; Martin, J. A.; Sinsko, J. A.; Summers, M. F. NMR and Computational Evidence that High Affinity Bradykinin Receptor Antagonists Adopt C-terminal β-turns. *J. Med. Chem.* **1993**, *36*. 1450–1460.

(21) Farmer, S. G.; Burch, R. M.; Dehaas, C. J.; Togo, J.; Steranka, L. R. [Arg^1, $DPhe^7$]-Substituted Analogues of Bradykinin Inhibit Vasopressin- and Bradykinin-Induced Contractions of Uterine Smooth Muscle. *J. Pharmacol. Exp. Ther.* **1989**, *248*, 677–681.

(22) Tissue strips were prepared as described elsewhere.[23] Cumulative dose–response curves were constructed to bradykinin in the absence and in the presence of increasing concentrations of bradykinin antagonists (0.1–0.3 μM). The EC_{50} of bradykinin was ca. 20 nM.

(23) Noronha-Blob, L.; Sturm, B. L.; Lowe, V. C.; Jackson, K. N.; Kachur, J. F. In Vitro and In Vivo Antimuscarinic Effects of (-)-*cis*-2,3-dihydro-3-(4-methylpiperazinylmethyl)-2-phenyl-1,5-benzothiazepin-4-(5H)one HCL (BTM-1086) in Guinea Pig Peripheral Tissues. *Life Sci.* **1990**, *46*, 1223–1231.

(24) Merrifield, R. B. Solid phase peptide synthesis. I. The Synthesis of a Tetrapeptide. *J. Am. Chem. Soc.* **1963**, *85*, 2149–2154.

(25) Vincent, M.; Remond, G.; Portevin, B.; Serkiz, B.; Laubie, M. Stereoselective Synthesis of a New Perhydroindole Derivative of Chiral Iminodiacids, a Potent Inhibitor of Angiotensin Converting Enzyme. *Tetrahedron Lett.* **1982**, *23*, 1677–1680.

(26) Stewart, J. M.; Young, J. D. Solid Phase Peptide Synthesis, 2nd ed.; Pierce Chemical Company: Rockford, IL, 1984.